The Hajdu Cheney mutation sensitizes mice to the osteolytic actions of tumor necrosis factor α

Received for publication, June 18, 2019, and in revised form, July 29, 2019 Published, Papers in Press, August 1, 2019, DOI 10.1074/jbc.RA119.009824

Jungeun Yu[‡§] and **Ernesto Canalis**[‡§¶1]

From the Departments of [‡]*Orthopaedic Surgery and* [¶]*Medicine,* [§]*UConn Musculoskeletal Institute, UConn Health, Farmington, Connecticut 06030*

Edited by Jeffrey E. Pessin

Hajdu Cheney syndrome (HCS) is characterized by craniofacial developmental abnormalities, acro-osteolysis, and osteoporosis and is associated with gain–of–NOTCH2 function mutations. A mouse model of HCS termed *Notch2*$^{tm1.1Ecan}$ harboring a mutation in exon 34 of *Notch2* replicating the one found in HCS was used to determine whether the HCS mutation sensitizes the skeleton to the osteolytic effects of tumor necrosis factor α (TNFα). TNFα injected over the calvarial vault caused a greater increase in osteoclast number, osteoclast surface, and eroded surface in *Notch2*$^{tm1.1Ecan}$ mice compared with littermate WT controls. Accordingly, the effect of TNFα on osteoclastogenesis was greatly enhanced in cultures of bone marrow–derived macrophages (BMMs) from *Notch2*$^{tm1.1Ecan}$ mice when compared with the activity of TNFα in control cultures. TNFα induced the expression of *Notch2* and *Notch2* mutant mRNA by ~2-fold, possibly amplifying the NOTCH2-dependent induction of osteoclastogenesis. The effect of TNFα on osteoclastogenesis in *Notch2*$^{tm1.1Ecan}$ mutants depended on NOTCH2 activation because it was reversed by anti-NOTCH2 negative regulatory region and anti-jagged 1 antibodies. The inactivation of *Hes1* prevented the TNFα effect on osteoclastogenesis in the context of the *Notch2*$^{tm1.1Ecan}$ mutation. In addition, the induction of *Il1b*, but not of *Tnfa* and *Il6*, mRNA by TNFα was greater in *Notch2*$^{tm1.1Ecan}$ BMMs than in control cells, possibly contributing to the actions of TNFα and NOTCH2 on osteoclastogenesis. In conclusion, the HCS mutation enhances TNFα-induced osteoclastogenesis and the inflammatory bone-resorptive response possibly explaining the acro-osteolysis observed in affected individuals.

NOTCH receptors 1–4 are single-pass type I transmembrane proteins that play a central role in cell fate determination and function (1, 2). In the skeleton, Notch signaling regulates development and homeostasis by controlling the differentiation and function of bone cells, including osteoblasts, osteoclasts, chondrocytes, and osteocytes (3–9). In mammals, there are five ligands for the Notch receptors: namely jagged (JAG)1, JAG2, delta-like (DLL)1, DLL3, and DLL4 (10). Activation of NOTCH receptors follows their interactions with ligands on adjacent cells, resulting in the cleavage of NOTCH by a disintegrin and metalloprotease (ADAM) and the γ-secretase complex and the release of the NOTCH intracellular domain (NICD)[2] (11, 12). The NICD translocates into the nucleus to form a complex with mastermind-like and recombination signal-binding protein for the immunoglobulin κ region (RBPJκ) and induce the expression of its target genes hairy enhancer of split (*Hes*) and HES-related with YRPW motif (*Hey*) (2, 13, 14 Although NOTCH receptors share structural and some biological functions, it is important to note that each NOTCH receptor exerts distinct effects on the skeleton; these are in part related to specific patterns of cellular expression of each receptor (11).

Hajdu Cheney syndrome (HCS) is a rare inherited disease characterized by craniofacial developmental abnormalities, acro-osteolysis, short stature, and osteoporosis (15–17). HCS is caused by point mutations or short deletions in exon 34 of *NOTCH2* that lead to the creation of a stop codon upstream of the proline (P), glutamic acid (E), serine (S), and threonine (T)-rich (PEST) domain (18–22). The PEST domain is recognized by the E3 ligase complex for ubiquitin-mediated degradation of NOTCH2. Therefore, the mutations result in the translation of a truncated NOTCH2 protein resistant to ubiquitin-dependent degradation and a gain–of–NOTCH2 function (23). To investigate the mechanisms responsible for HCS, we created a mouse model termed *Notch2*$^{tm1.1Ecan}$ harboring a point mutation (6955C→T) in exon 34 of *Notch2* upstream of the PEST domain. Heterozygous *Notch2*$^{tm1.1Ecan}$ mice exhibit cancellous and cortical bone osteopenia due to increased osteoclast number and bone resorption (5). *Notch2*$^{tm1.1Ecan}$ mice also display a reallocation of B cells to the marginal zone of the spleen, shortening of the limbs, and sensitization to the development of osteoarthritis in destabilized joints (24, 25). This is possibly because of increased expression of interleukin (IL) 6, revealing

This work was supported by National Institutes of Health Grant AR068160 from NIAMS and Grant DK045227 from NIDDK. The authors declare that they have no conflicts of interest with the contents of this article. The content is solely the responsibility of the authors and does not necessarily represent the official views of the National Institutes of Health.

[1] To whom correspondence should be addressed. Tel.: 860-679-7978; Fax: 860-679-1474; E-mail: canalis@uchc.edu.

[2] The abbreviations used are: NICD, NOTCH intracellular domain; α-MEM, α-minimum essential medium; BMM, bone marrow-derived macrophage; CMV, cytomegalovirus; ES/BS, eroded surface/bone surface; FBS, fetal bovine serum; HCS, Hajdu Cheney syndrome; IL, interleukin; M-CSF, macrophage colony-stimulating factor; m.o.i., multiplicity of infection; NF-κB, nuclear factor-κB; NRR, negative regulatory region; N.Oc/B.Pm, number of osteoblasts/bone perimeter; Oc.S/BS, osteoclast surface/bone surface; PEST, proline (P), glutamic acid (E), serine (S), and threonine (T)-rich; qRT-PCR, quantitative reverse transcription-PCR; RANKL, receptor activator of NF-κB ligand; RBPJκ, recombination signal-binding protein for immunoglobulin κ region; TNFα, tumor necrosis factor α; TRAP, tartrate-resistant acid phosphatase; Veh, vehicle control; PI3K, phosphoinositol 3-kinase.

a propensity to an enhanced inflammatory response (24). *Notch2*$^{tm1.1Ecan}$ does not exhibit apparent acro-osteolysis, and homozygous mice display craniofacial dysmorphism and newborn lethality.[3] The skeletal phenotype of *Notch2*$^{tm1.1Ecan}$ reproduces the human syndrome, and iliac crest biopsies from humans afflicted by HCS reveal osteopenia and trabecularization of cortical bone (26).

Histological examination of biopsies from the acro-osteolysis lesions in subjects with HCS reveal the presence of an inflammatory process and neovascularization, but the mechanisms responsible for the bone lysis are not known (17, 27-29). Tumor necrosis factor α (TNFα) is a proinflammatory cytokine primarily produced by activated macrophages. TNFα induces gene expression of *Il6* and *Il1b* as well as its own expression (30, 31). TNFα, IL6, and IL1β enhance the differentiation of cells of the myeloid lineage toward osteoclasts and increase the bone-resorbing activity of mature osteoclasts (32–39).

The excessive release of TNFα, IL6, and IL1β during the inflammatory response perturbs bone homeostasis and promotes pathologic bone erosion and may be mechanistically involved in the acro-osteolysis of HCS (40–42). Therefore, we asked the question whether the HCS mutation sensitizes the skeleton to the osteolytic actions of TNFα. To this end, we examined the effects of TNFα on bone resorption *in vivo* and on osteoclastogenesis *in vitro* in *Notch2*$^{tm1.1Ecan}$ mice and mechanisms responsible. Because we have found no differences in phenotypic manifestations between male and female *Notch2*$^{tm1.1Ecan}$ mice, the studies were conducted in male mice and sex-matched littermate controls.

Results

Hajdu Cheney Notch2$^{tm1.1Ecan}$ *mutation enhances TNFα-induced osteolysis in calvarial bone*

To examine whether the Hajdu Cheney mutation sensitizes mice to the osteolytic actions of TNFα, *Notch2*$^{tm1.1Ecan}$ mice and control littermates were administered TNFα or PBS as a vehicle control by subcutaneous injection over the calvarial vault once a day for 4 days. Tartrate-resistant acid phosphatase (TRAP)/hematoxylin-stained calvarial sections revealed that TNFα administration increased the number of TRAP-positive multinucleated cells and osteolysis in *Notch2*$^{tm1.1Ecan}$ and littermate control mice. The effect was more pronounced in *Notch2*$^{tm1.1Ecan}$ mice, and osteoclast number, osteoclast surface, and eroded surface were 1.7-fold higher in *Notch2*$^{tm1.1Ecan}$ calvarial bones than in controls (Fig. 1).

Hajdu Cheney mutation enhances TNFα-induced osteoclastogenesis in vitro

TNFα acts directly and indirectly to induce osteoclastogenesis by promoting the osteoclastogenic potential of osteoclast precursors and by increasing receptor activator of NF-κB (NF-κB) ligand (RANKL) expression in osteoblasts (43, 44). To confirm a direct effect of TNFα on osteoclastogenesis in the context, or not, of the Hajdu Cheney mutation, bone marrow-derived macrophages (BMMs) from *Notch2*$^{tm1.1Ecan}$ and control littermates were cultured in the presence of macrophage colony-stimulating factor (M-CSF) and TNFα. The effect of TNFα on osteoclastogenesis was enhanced in cultures of *Notch2*$^{tm1.1Ecan}$ BMMs compared with the effects of TNFα in control cultures (Fig. 2). Although *Notch2*$^{tm1.1Ecan}$ BMMs were sensitized to the action of TNFα, there was no difference in *Tnfr1* and *Tnfr2* mRNA expression between *Notch2*$^{tm1.1Ecan}$ and control mice either *in vivo* in calvariae or *in vitro* in BMM cultures (Fig. 3). The effect of TNFα on early signal activation of mitogen-activated protein kinases and IκBα was comparable between *Notch2*$^{tm1.1Ecan}$ and control BMMs, although a greater induction of AKT phosphorylation was observed in *Notch2*$^{tm1.1Ecan}$ cultures than in control cultures treated with TNFα (Fig. 3). TNFα treatment induced NF-κB activation in BMMs of both genotypes, as defined by enhanced NF-κB binding to consensus DNA sequences, but there was no difference in NF-κB activation between *Notch2*$^{tm1.1Ecan}$ and control BMM cultures (Fig. 3). The results suggest that the enhanced osteoclastogenic response of *Notch2*$^{tm1.1Ecan}$ cells to TNFα was inde-

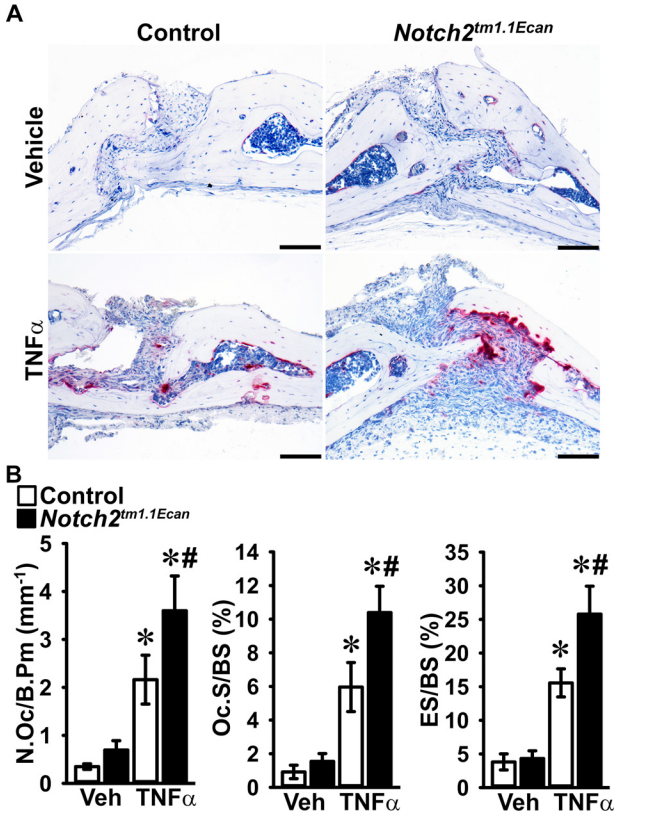

Figure 1. Hajdu Cheney mice display greater osteoclast number and eroded surface than littermate controls following TNFα treatment. Calvarial bones of *Notch2*$^{tm1.1Ecan}$ and sex-matched littermate control mice were administered 2 μg TNFα or PBS (vehicle, *Veh*) once a day for 4 days over the calvarial vault by subcutaneous injection. *A,* representative images of histological sections of calvariae stained with TRAP and hematoxylin showing increased number of osteoclasts and eroded surface in TNFα-treated *Notch2*$^{tm1.1Ecan}$ mice. The *scale bars* in the *right corner* represent 100 μm. *B,* bone histomorphometric analysis of the calvarial bones from *Notch2*$^{tm1.1Ecan}$ (*black bars*) mutant mice and littermate controls (*white bars*). Values are means ± S.D.; vehicle $n = 4$ and TNFα $n = 8$ biological replicates for control and *Notch2*$^{tm1.1Ecan}$ mice, respectively. Parameters shown are as follows: number of osteoclasts/bone perimeter (*N.Oc/B.Pm*); osteoclast surface/bone surface (*Oc.S/BS*); eroded surface/bone surface (*ES/BS*). *, significantly different between TNFα and vehicle, $p < 0.05$. #, significantly different between *Notch2*$^{tm1.1Ecan}$ and control, $p < 0.05$.

[3] E. Canalis, unpublished observations.

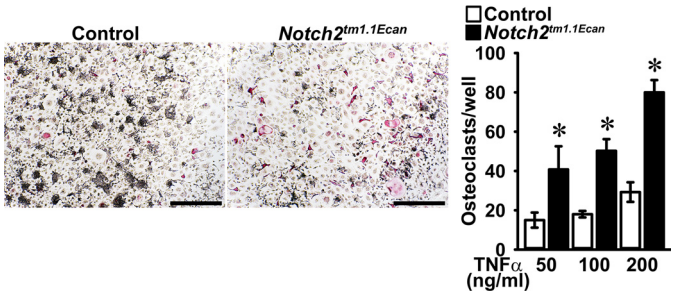

Figure 2. Hajdu Cheney mutant BMMs are sensitized to the action of TNFα on osteoclastogenesis. BMMs derived from 2-month-old *Notch2*$^{tm1.1Ecan}$ mice and control littermates were cultured in the presence of M-CSF at 30 ng/ml and of TNFα at 50, 100, and 200 ng/ml for 6 days. Cells were stained with TRAP, and representative images of TRAP-stained multinucleated cells are shown. The *scale bar* in the *right corner* represents 500 μm. TRAP-positive cells with more than three nuclei were considered osteoclasts, and values are means ± S.D.; $n = 4$ biological replicates for control (*white bars*) and *Notch2*$^{tm1.1Ecan}$ (*black bars*) cells. *, significantly different between *Notch2*$^{tm1.1Ecan}$ and control, $p < 0.05$.

pendent of NF-κB activation and possibly related to enhanced AKT phosphorylation.

TNFα promotes the expression of Notch2 and proinflammatory cytokines

To test for the acute effect of TNFα on gene expression, BMMs from *Notch2*$^{tm1.1Ecan}$ mice and control littermates were treated with TNFα for 6 and 18 h. TNFα induced the expression of *Notch2* mRNA in *Notch2*$^{tm1.1Ecan}$ and control BMMs. *Notch2* mutant (*Notch2*$^{6955C\rightarrow T}$) transcripts were detected only in *Notch2*$^{tm1.1Ecan}$ cells, and their expression was enhanced by TNFα. *Hes1* mRNA levels were significantly increased in *Notch2*$^{tm1.1Ecan}$ BMMs, but they were not affected by treatment with TNFα. The expression of *Tnfa*, *Il6*, and *Il1b* was significantly increased by TNFα, but only the induction of *Il1b* was greater in *Notch2*$^{tm1.1Ecan}$ BMMs than in control cultures (Fig. 4). To examine for changes in gene expression during TNFα-induced osteoclast differentiation, *Notch2*$^{tm1.1Ecan}$ and control BMMs were cultured in the presence of M-CSF and TNFα for 3 and 6 days. TNFα induced *Notch2* and *Notch2*$^{6955C\rightarrow T}$ transcripts by up to 2-fold. *Hes1* mRNA expression was increased in *Notch2*$^{tm1.1Ecan}$ cells but was not altered by TNFα (Fig. 5). TNFα induced *Tnfa*, *Il6*, and *Il1b* in both *Notch2*$^{tm1.1Ecan}$ and control osteoclasts, but only *Il1b* was increased in *Notch2*$^{tm1.1Ecan}$ osteoclasts to a greater extent than in control cells (Fig. 5). Osteoclastogenic gene markers, such as *Acp5* and *Ctsk*, were up-regulated during TNFα-induced osteoclastogenesis and were significantly greater in *Notch2*$^{tm1.1Ecan}$ osteoclasts than in control cells (Fig. 5). The NF-κB– dependent *Nfatc1* gene was up-regulated by TNFα; but in accordance with the results on NF-κB activation, its induction was of equal magnitude in control and *Notch2*$^{tm1.1Ecan}$ cells.

TNFα accelerates NOTCH2 signal activation and increases JAG1 expression

NOTCH signaling is activated following interactions with ligands of the JAG and DLL families. In previous work, we found that *Jag1*, but not *Jag2* or *Dll1*, *Dll3*, and *Dll4* transcripts, is expressed as BMMs differentiate toward osteoclasts (11). *Jag1* mRNA and JAG1 protein levels were increased about 1.4- and 3-fold, respectively, during TNFα-induced osteoclastogenesis, but the induction was of equal magnitude in *Notch2*$^{tm1.1Ecan}$ and control osteoclasts (Fig. 6). In accordance with the increase in *Notch2* mRNA during osteoclastogenesis, the levels of NOTCH2 were increased as BMMs matured as osteoclasts in the presence of TNFα. The NOTCH2 intracellular domain (N2ICD), representative of NOTCH2 signal activation and cleavage of NOTCH2, was increased in *Notch2*$^{tm1.1Ecan}$ and control osteoclasts following TNFα treatment. Although N2ICD was increased in both *Notch2*$^{tm1.1Ecan}$ and control cells, the truncated form of NOTCH2, lacking the PEST domain (N2ICD$^{\Delta PEST}$), was only detected in *Notch2*$^{tm1.1Ecan}$ cells and increased during differentiation. Therefore, the total levels of N2ICD, intact and truncated, were 2-fold greater in *Notch2*$^{tm1.1Ecan}$ cells than in control cells (Fig. 6). HES1 levels were 2-fold greater in *Notch2*$^{tm1.1Ecan}$ cultures, but NFATc1 was increased to an equal extent in *Notch2*$^{tm1.1Ecan}$ and control cultures as they differentiated toward osteoclasts in the presence of TNFα (Fig. 6).

Preventing NOTCH2 signaling reverses the sensitizing effect of the Hajdu Cheney mutation on TNFα-induced osteoclastogenesis

To determine whether preventing NOTCH2 signal activation can reverse the effect of the *Notch2*$^{tm1.1Ecan}$ mutation on TNFα-induced osteoclastogenesis, BMMs from *Notch2*$^{tm1.1Ecan}$ mice and control littermates were cultured in the presence of M-CSF and TNFα with antibodies directed to the NRR of NOTCH2 or with anti-JAG1 antibodies (45–47). TNFα induced osteoclastogenesis in *Notch2*$^{tm1.1Ecan}$ BMMs by ~1.6–1.7-fold, an effect that was reversed by anti-NOTCH2 NRR and by anti-JAG1 antibodies (Fig. 7). Moreover, anti-JAG1 antibodies reduced osteoclast differentiation in control as well as in *Notch2*$^{tm1.1Ecan}$ cultures treated with TNFα, demonstrating that NOTCH signal activation is a requirement for TNFα-dependent osteoclastogenesis (Fig. 7).

Inactivation of Hes1 reverses the sensitizing effect of the Hajdu Cheney mutation on TNFα-induced osteoclastogenesis

In preliminary experiments, we demonstrated that *Hes1* is expressed in BMMs, and its expression increases during osteoclastogenesis, whereas *Hey1*, *Hey2*, and *HeyL* transcripts are not detected in this cell lineage (11). To examine the effect of HES1 on osteoclastogenesis in *Notch2*$^{tm1.1Ecan}$ cells, osteoclast precursors from *Notch2*$^{tm1.1Ecan}$;*Hes1*$^{loxP/loxP}$ and *Hes1*$^{loxP/loxP}$ littermate controls were transduced with adenoviruses carrying CMV-Cre (Ad-Cre) or GFP (Ad-GFP) control vectors. *Hes1* mRNA levels were decreased by 55–80% in *Notch2*$^{tm1.1Ecan}$;*Hes1*$^{\Delta/\Delta}$ and *Hes1*$^{\Delta/\Delta}$ osteoclasts transduced with Ad-Cre compared with *Notch2*$^{tm1.1Ecan}$;*Hes1*$^{loxP/loxP}$ and *Hes1*$^{loxP/loxP}$ cells transduced with Ad-GFP. *Notch2* and *Notch2*$^{6955C\rightarrow T}$ mutant transcripts were not affected by the *Hes1* inactivation, whereas the down-regulation of *Hes1* decreased the *Il1b* induction observed in *Notch2*$^{tm1.1Ecan}$ cells (Fig. 8). *Notch2*$^{tm1.1Ecan}$;*Hes1*$^{loxP/loxP}$ osteoclast precursors treated with TNFα exhibited a 1.5-fold increase in osteoclast number compared with *Hes1*$^{loxP/loxP}$ cells. Osteoclast number was decreased by 60% in *Notch2*$^{tm1.1Ecan}$;*Hes1*$^{\Delta/\Delta}$ and decreased by about 30% in

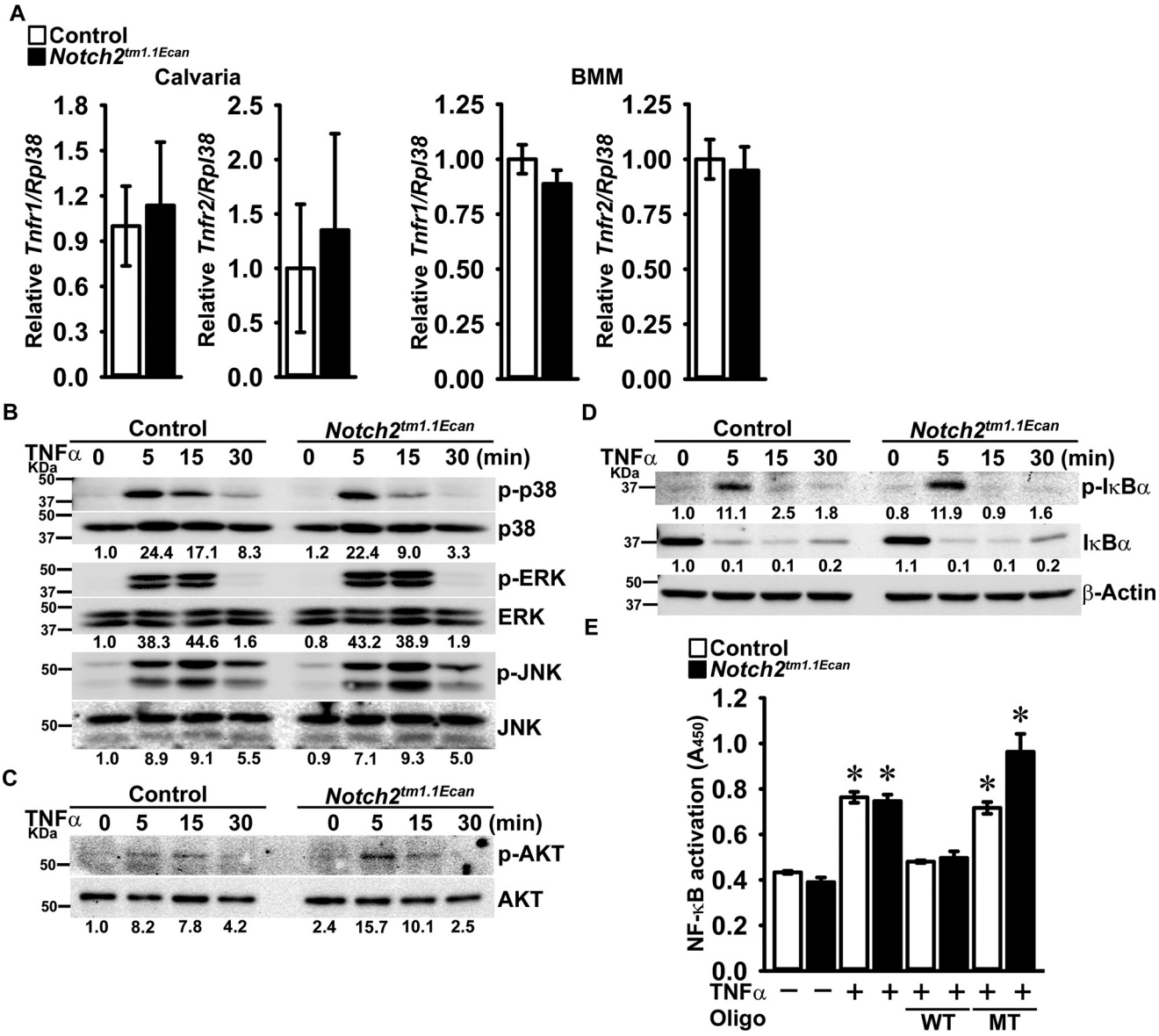

Figure 3. TNFα receptor expression and TNFα-induced early signal activation are not altered in Hajdu Cheney mutants. *A,* total RNA was extracted from calvarial bones (*left*) or BMMs (*right*) of *Notch2*$^{tm1.1Ecan}$ and sex-matched littermate control mice and examined for relative *Tnfr1* and *Tnfr2* gene expression by qRT-PCR, corrected for *Rpl38* copy number. Values are means ± S.D.; $n = 4$ biological replicates for control (*white bars*) and *Notch2*$^{tm1.1Ecan}$ (*black bars*) calvarial bones or BMMs. *B–D,* BMMs derived from 2-month-old *Notch2*$^{tm1.1Ecan}$ mice and control littermates were cultured for 2 h in the absence of serum and exposed to TNFα at 200 ng/ml for the indicated periods of time, and whole-cell lysates (35 μg of total protein except panel *C*, 15 μg of total protein for C) were examined by immunoblotting. *B*, using anti-p-p38, p-ERK, and p-JNK antibodies, stripped and reprobed with anti-p38, ERK, and JNK antibodies. *C*, using anti-p-AKT antibodies and reprobed with anti-AKT antibodies. *D*, using anti-p-IκBα or β-Actin antibodies, stripped and reprobed with IκBα antibodies. The band intensity was quantified by ImageLab™ software (version 5.2.1), and the numerical ratios of phosphorylated/unphosphorylated signal in *B* and *C* or of p-IκBα/β-Actin and of IκBα/β-Actin in *D* are shown *below* each blot. Control ratios at day 0 are normalized to 1. *E,* BMMs from 2-month-old *Notch2*$^{tm1.1Ecan}$ mice and control littermates were cultured for 2 h in the absence of serum and exposed to TNFα at 200 ng/ml for 1 h. 20 μg of nuclear extracts for each sample were examined by TransAM™ Flexi NF-κB p65 activation assay kit, and colorimetric changes were measured at 450 nm. Values are means ± S.D.; $n = 3$ technical replicates for control (*white bars*) and *Notch2*$^{tm1.1Ecan}$ (*black bars*) BMMs. *, significantly different compared with control without TNFα, $p < 0.05$.

Hes1$^{\Delta/\Delta}$ cells so that the *Hes1* inactivation reversed the TNFα effect on osteoclastogenesis in the context of the *Notch2*$^{tm1.1Ecan}$ mutation and reduced the effect of TNFα in control cultures (Fig. 8).

Preventing NOTCH2 signaling reverses the sensitizing effect of the Hajdu Cheney mutation on TNFα-induced osteolysis

To examine whether preventing NOTCH2 signal activation can reverse the effect of the *Notch2*$^{tm1.1Ecan}$ mutation on TNFα-induced osteolysis, *Notch2*$^{tm1.1Ecan}$ mice and control littermates were administered anti-NOTCH2 NRR or control anti-ragweed antibodies with TNFα by subcutaneous injection over the calvarial vault once a day for 4 days. TRAP/hematoxylin-stained calvarial sections revealed that osteoclast number, osteoclast surface, and eroded surface were 2-fold higher in TNFα-treated *Notch2*$^{tm1.1Ecan}$ calvarial bones than in TNFα-treated WT controls. The effect of the *Notch2*$^{tm1.1Ecan}$ mutation was reversed by the administration of anti-NOTCH2 NRR antibodies, and osteoclast number, osteoclast surface, and eroded surface were significantly reduced compared with anti-

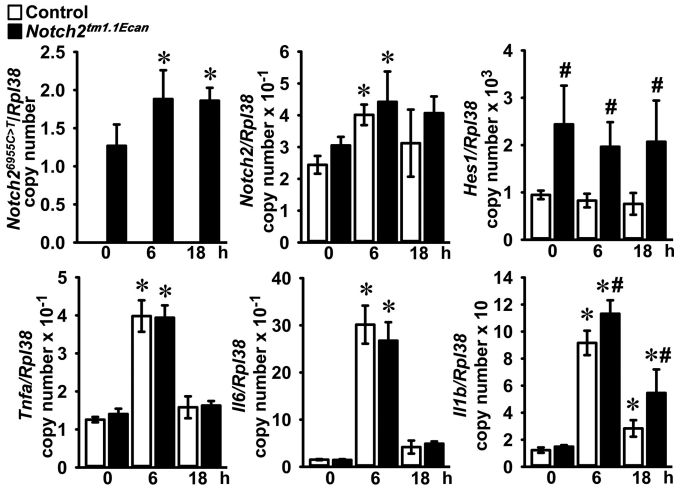

Figure 4. TNFα enhances the expression of *Notch2* and proinflammatory cytokines in Hajdu Cheney mutant and control BMMs. BMMs derived from 2-month-old *Notch2*$^{tm1.1Ecan}$ mice and control littermates were cultured for the indicated periods of time in the presence of M-CSF at 30 ng/ml and TNFα at 200 ng/ml. Total RNA was extracted, and gene expression was determined by qRT-PCR. Data are expressed as *Notch2*$^{6955C\rightarrow T}$, *Notch2*, *Hes1*, *Tnfa*, *Il6*, and *Il1b*, corrected for *Rpl38* copy number. Values are means ± S.D.; $n = 4$ biological replicates for control (*white bars*) and *Notch2*$^{tm1.1Ecan}$ (*black bars*) BMMs. *, significantly different compared with time 0, $p < 0.05$. #, significantly different between *Notch2*$^{tm1.1Ecan}$ and control, $p < 0.05$.

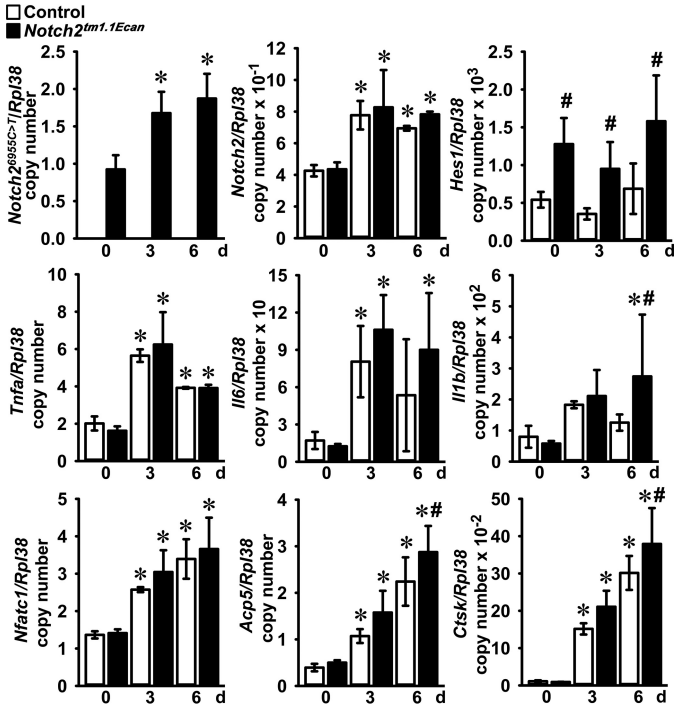

Figure 5. Expression of *Notch2* and proinflammatory cytokines is increased during TNFα-induced osteoclastogenesis. BMMs derived from 2-month-old *Notch2*$^{tm1.1Ecan}$ mice and control littermates were cultured in the presence of M-CSF at 30 ng/ml and TNFα at 200 ng/ml for 6 days. Total RNA was extracted, and gene expression was determined by qRT-PCR. Data are expressed as *Notch2*$^{6955C\rightarrow T}$, *Notch2*, *Hes1*, *Tnfa*, *Il6*, *Il1b*, *Nfatc1*, *Acp5*, and *Ctsk*, corrected for *Rpl38* copy number. Values are means ± S.D.; $n = 4$ biological replicates for control (*white bars*) and *Notch2*$^{tm1.1Ecan}$ (*black bars*) cells. *, significantly different compared with day 0, $p < 0.05$. #, significantly different between *Notch2*$^{tm1.1Ecan}$ and control, $p < 0.05$.

ragweed–treated *Notch2*$^{tm1.1Ecan}$ mice (Fig. 9). As a consequence, osteoclast number and surface were no longer different between TNFα-treated *Notch2*$^{tm1.1Ecan}$ and control mice; the anti-NOTCH2 NRR antibody also reduced eroded surface in control mice (Fig. 9).

Notch2$^{tm1.1Ecan}$ mice have normal serum TNFα levels

To determine whether mice harboring the *Notch2*$^{tm1.1Ecan}$ mutation have altered serum levels of TNFα, serum was obtained from *Notch2*$^{tm1.1Ecan}$ and control littermates. At 2 months of age, serum TNFα was (means ± S.D.; $n = 3–4$) 15.5 ± 0.2 pg/ml in control and 15.3 ± 0.1 pg/ml in *Notch2*$^{tm1.1Ecan}$ mice; at 12 months of age TNFα was 15.8 ± 0.4 pg/ml in control and 15.6 pg/ml in *Notch2*$^{tm1.1Ecan}$ mice (both $p > 0.05$).

Discussion

In this study, we demonstrated that the TNFα-induced osteoclastogenesis and the inflammatory bone-resorptive response to TNFα are enhanced in a mouse model of HCS (Fig. 10). The effect of TNFα required the activation of NOTCH2 signaling because it was reversed *in vitro* and *in vivo* by anti-NOTCH2 NRR and by anti-JAG1 antibodies. Moreover, anti-JAG1 antibodies inhibited control and *Notch2*$^{tm1.1Ecan}$ mutant-dependent osteoclastogenesis demonstrating that NOTCH activation is necessary for optimal osteoclast differentiation secondary to TNFα.

A limitation of the *in vivo* experiments is that they were conducted in male *Notch2*$^{tm1.1Ecan}$ and sex-matched controls, and as a consequence caution should be exerted before extrapolating the results to female mice. Recently, an alternative mouse model of HCS with a *6272delT* in exon 34 of *Notch2* was reported, and mice were studied up to 12 months of age (48). Like *Notch2*$^{tm1.1Ecan}$ mutants, these mice developed osteopenia secondary to increased bone resorption; the major difference between *Notch2*$^{tm1.1Ecan}$ and mice harboring the *6272delT* mutation is that the latter exhibit increased bone formation and high bone turnover (48). Neither mouse model exhibited acro-osteolysis. This could suggest that environmental factors or vascular injury are required in addition to the inflammatory component for the development of acro-osteolysis. These additional factors do not seem to occur in the available mouse models of the disease that are suitable to examine the inflammatory component of the syndrome but not the fully established acro-osteolysis.

Our results are in contrast to previous work demonstrating that RBPJκ, a component of Notch canonical signaling, inhibits TNFα-induced osteoclastogenesis by suppressing *Nfatc1* (49). It is possible that RBPJκ acts directly on osteoclastogenesis and independently of Notch signaling or that the effects of NOTCH2 and HES1 on osteoclastogenesis are independent of canonical Notch signaling. However, we and others have consistently demonstrated a stimulatory effect of NOTCH2 on osteoclastogenesis that is congruent with the results observed in this work (5, 7, 23).

NOTCH activation results in the induction of *Hes* and *Heys*, and cells of the osteoclast lineage express *Hes1* and low levels of *Hes3* and *Hes5* mRNA but do not express *Hey1*, *Hey2*, or *HeyL* transcripts (11). *Hes1* expression levels were increased in *Notch2*$^{tm1.1Ecan}$ mutant cells and played a role in the TNFα-mediated osteoclastogenic effect because this was no longer

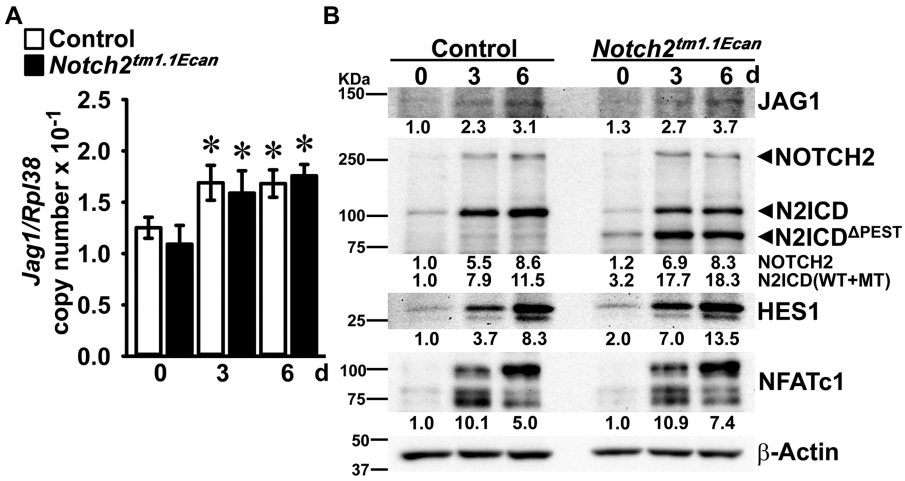

Figure 6. TNFα accelerates NOTCH2 signal activation during osteoclast differentiation and enhances JAG1 expression. BMMs derived from 2-month-old *Notch2*$^{tm1.1Ecan}$ mice and control littermates were cultured in the presence of M-CSF at 30 ng/ml and of TNFα at 200 ng/ml for 6 days. *A,* total RNA was extracted, and gene expression was determined by qRT-PCR. Data are expressed as *Jag1*, corrected for *Rpl38* copy number. Values are means ± S.D.; $n = 4$ biological replicates for control (*white bars*) and *Notch2*$^{tm1.1Ecan}$ (*black bars*) cells. *, significantly different compared with day 0, $p < 0.05$. *B,* whole-cell lysates (35 μg of total protein) were examined by immunoblotting using anti-JAG1, NOTCH2 and N2ICD, HES1, NFATc1, and β-Actin antibodies. The band intensity was quantified by ImageLab™ software (version 5.2.1), and the numerical ratio of JAG1/β-Actin, NOTCH2/β-Actin, N2ICD (including N2ICD$^{\Delta PEST}$)/β-Actin, HES1/β-Actin, and NFATc1/β-Actin is shown *below* each blot. All control ratios at day 0 are normalized to 1.

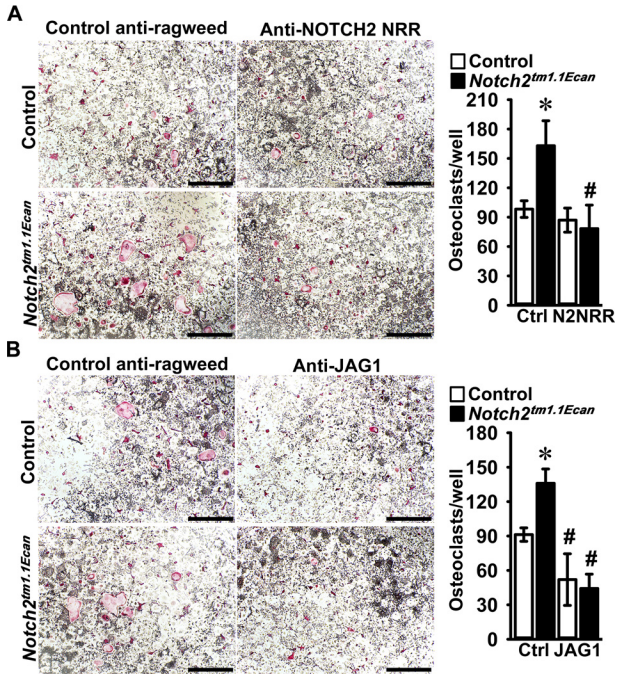

Figure 7. Preventing NOTCH2 signal activation reverses the effect of the Hajdu Cheney mutation on TNFα-induced osteoclastogenesis. BMMs derived from 2-month-old *Notch2*$^{tm1.1Ecan}$ mice and control littermates were cultured with M-CSF at 30 ng/ml and TNFα at 200 ng/ml in the presence of control anti-ragweed at 10 or 20 μg/ml (*Ctrl*) or anti-NOTCH2 NRR (*N2NRR*) at 10 μg/ml (*A*), or anti-JAG1 (JAG1) at 20 μg/ml (*B*) for 6 days. *A* and *B,* representative images of TRAP-stained multinucleated cells obtained after 6 days of culture are shown. The *scale bars* in the *right corners* represent 500 μm. TRAP-positive cells with more than three nuclei were considered as osteoclasts, and values are means ± S.D. (*top* and *bottom right*); $n = 4$ biological replicates for control (*white bars*) and *Notch2*$^{tm1.1Ecan}$ (*black bars*). *, significantly different between *Notch2*$^{tm1.1Ecan}$ and control, $p < 0.05$. #, significantly different between anti-NOTCH2 NRR or anti-JAG1 and control anti-ragweed antibodies, $p < 0.05$.

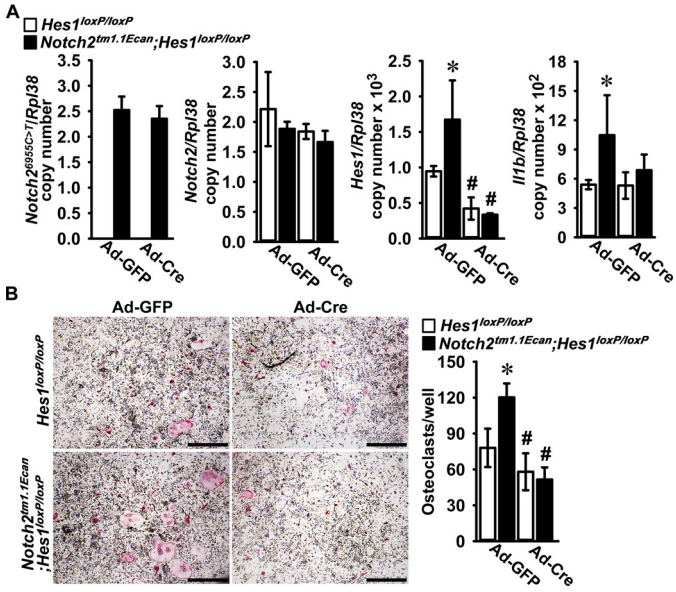

Figure 8. Hes1 inactivation reverses the effect of the Hajdu Cheney mutation on TNFα-induced osteoclastogenesis. Osteoclast precursors derived from 2-month-old *Notch2*$^{tm1.1Ecan}$;*Hes1*$^{loxP/loxP}$ and *Hes1*$^{loxP/loxP}$ littermate controls were transduced with adenoviruses carrying CMV-Cre (*Ad-Cre*) or GFP (*Ad-GFP*) as control at m.o.i. 100 and cultured with M-CSF at 30 ng/ml and TNFα at 200 ng/ml for 3 days until the formation of multinucleated TRAP-positive cells. *A,* total RNA was extracted, and gene expression was determined by qRT-PCR. Data are expressed as *Notch2*$^{6955C\rightarrow T}$, *Notch2*, *Hes1*, and *Il1b*, corrected for *Rpl38* copy number. Values are means ± S.D.; $n = 4$ technical replicates for *Hes1*$^{loxP/loxP}$ (*white bars*) and *Notch2*$^{tm1.1Ecan}$;*Hes1*$^{loxP/loxP}$ (*black bars*) cells transduced with Ad-Cre or Ad-GFP. *B,* representative images of TRAP-stained multinucleated cells are shown. The *scale bars* in the *right corner* represent 500 μm. TRAP-positive cells with more than three nuclei were considered osteoclasts, and values are means ± S.D.; $n = 4$ technical replicates for *Hes1*$^{loxP/loxP}$ (*white bars*) and *Notch2*$^{tm1.1Ecan}$;*Hes1*$^{loxP/loxP}$ (*black bars*) transduced with Ad-Cre or Ad-GFP. *, significantly different between *Notch2*$^{tm1.1Ecan}$;*Hes1*$^{loxP/loxP}$ and *Hes1*$^{loxP/loxP}$ control, $p < 0.05$. #, significantly different between Ad-Cre and Ad-GFP, $p < 0.05$.

detected following the inactivation of *Hes1.* Whereas HES1 plays an inhibitory role in osteoblast differentiation, and its overexpression in osteoblasts causes osteopenia, there is virtually no knowledge regarding its function in osteoclast differentiation or function (50). It is likely that HES1 plays a critical role in osteoclastogenesis and that its function is not limited to the osteoclastogenesis occurring during an inflammatory state.

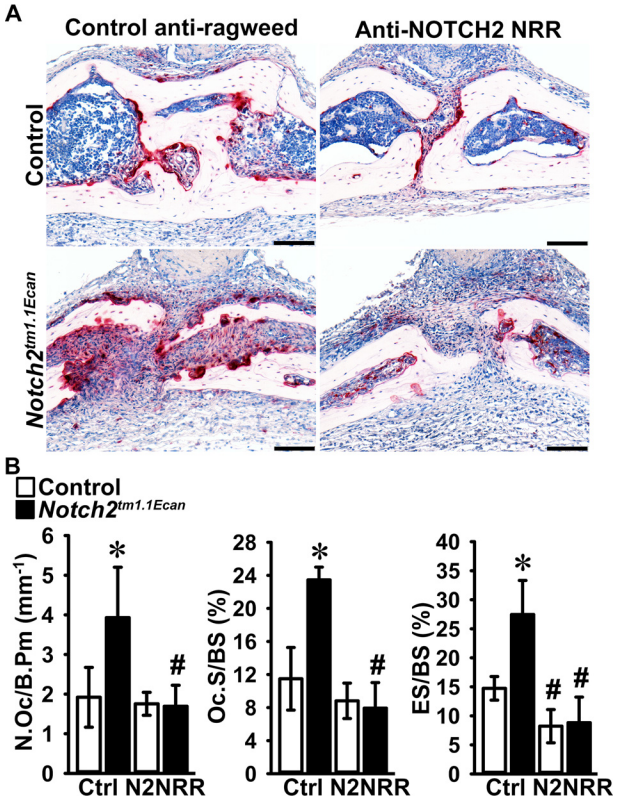

Figure 9. Preventing NOTCH2 signal activation reverses the effect of the Hajdu Cheney mutation on TNFα-induced osteolysis. Calvarial bones from *Notch2*$^{tm1.1Ecan}$ and sex-matched littermate control mice were administered 2 μg of TNFα with anti-NOTCH2 NRR or control anti-ragweed antibodies at a dose of 10 mg/kg once a day for 4 days over the calvarial vault by subcutaneous injection. *A,* representative images of histological sections of calvariae stained with TRAP and hematoxylin showing reversal of the TNFα-induced osteolysis in *Notch2*$^{tm1.1Ecan}$ mice by anti-NOTCH2 NRR antibodies. *Scale bars* in the *right corner* represent 100 μm. *B,* bone histomorphometric analysis of calvarial bones from *Notch2*$^{tm1.1Ecan}$ (*black bars*) mutant mice and littermate controls (*white bars*). Values are means ± S.D.; control anti-ragweed antibody (*Ctrl*) $n = 4–5$ and anti-NOTCH2 NRR (*N2NRR*) $n = 5$ biological replicates for control and *Notch2*$^{tm1.1Ecan}$ mice, respectively. Parameters shown are as follows: number of osteoclasts/bone perimeter (*N.Oc/B.Pm*); osteoclast surface/bone surface (*Oc.S/BS*); and eroded surface/bone surface (*ES/BS*). *, significantly different between *Notch2*$^{tm1.1Ecan}$ and control, $p < 0.05$. #, significantly different between anti-NOTCH2 NRR and control anti-ragweed antibodies, $p < 0.05$.

It has been reported that toll-like receptor signaling and pro-inflammatory cytokines, such as TNFα and IL1β, induce gene expression of NOTCH receptors and ligands as well as signal activation of NOTCH in several cells and tissues (51). TNFα increased the expression of JAG1 and NOTCH2 during osteoclast differentiation to a similar extent in *Notch2*$^{tm1.1Ecan}$ and control cells. However, only *Notch*$^{tm1.1Ecan}$ mutant cells synthesized the truncated form of N2ICD (N2ICD$^{\Delta PEST}$) and the intact N2ICD. The summation of the intact and truncated forms of N2ICD resulted in an ~2-fold greater expression of N2ICD in *Notch2*$^{tm1.1Ecan}$ mutants than in control cells. The N2ICD$^{\Delta PEST}$ is more stable than WT N2ICD because it is resistant to ubiquitin-mediated degradation, explaining the gain–of–NOTCH2 function and the *Hes1* induction in *Notch2*$^{tm1.1Ecan}$ cells (23, 52). The direct effects of NOTCH2 signaling and HES1 on TNFα-induced osteolysis and osteoclast differentiation in the context of the *Notch2*$^{tm1.1Ecan}$ mutation were reversed by treatment with anti-NOTCH2 NRR and anti-JAG1 antibodies and by the *Hes1* inactivation. Moreover, anti-JAG1 antibodies and the down-regulation of *Hes1* tempered the effects of TNFα in control cultures. This indicates that the effects of TNFα on osteoclastogenesis require NOTCH signal activation and HES1 expression.

Notch2$^{tm1.1Ecan}$ mutant cells displayed greater *Il1b* mRNA levels than control cells. The induction of *Il1b* was HES1-dependent, and this is in agreement with observations in alternative cellular systems (53). Notch signaling and HES1 inhibit the phosphatase and tensin homolog (PTEN) and as a consequence up-regulate the PI3K–AKT signaling pathway, and PI3K–AKT signaling enhances IL1β expression (54–56). In this study, we found greater induction of phospho-AKT by TNFα in *Notch2*$^{tm1.1Ecan}$ BMM cultures. Therefore, it is possible that HES1 signals through the PI3K–AKT pathway to enhance osteoclastogenesis and induce IL1β (57). IL1β is involved in the bone-resorbing activity of osteoclasts and in osteoclast formation (37). IL1β might accelerate TNFα-induced osteolysis by increasing the bone-resorbing activity of osteoclasts in *Notch2*$^{tm1.1Ecan}$ mice *in vivo* and contribute to the induction of *Hes1* mRNA, as was reported in chondrocytes (58).

RANKL and TNFα signaling activate transcription factor NF-κB. It has been reported that RANKL-induced N2ICD associates with p65 subunit of NF-κB to enhance the transcriptional activity of *Nfatc1* (7). We confirmed that TNFα induced NF-κB activation; however, this was not different between *Notch2*$^{tm1.1Ecan}$ and control cultures. In accordance with this finding, the expression of target genes dependent on NF-κB activation, including *Tnfa*, *Il6*, and *Nfatc1*, but not *Il1b*, was not different between *Notch2*$^{tm1.1Ecan}$ and control cultures treated with TNFα. This would suggest that mechanisms independent of NF-κB activation are responsible for the induction of IL1β as well as for the enhanced osteoclastogenic response of *Notch2*$^{tm1.1Ecan}$ mice to TNFα. This could entail either direct effects of the N2ICD or effects of HES1 on osteoclastogenesis, possibly by inducing AKT phosphorylation as a result of an inhibition of PTEN.

Serum levels of TNFα were not different between *Notch2*$^{tm1.1Ecan}$ and control mice. In addition, the serum from *Notch2*$^{tm1.1Ecan}$ and control mice was examined by Proteome Profiler Mouse Cytokine Array (R&D Systems, Minneapolis, MN) to address whether other proinflammatory cytokines were up-regulated in the systemic circulation of *Notch2*$^{tm1.1Ecan}$ mice. Few cytokines, including CXC motif chemokine ligand 13, complement component 5a, CD54, M-CSF, and stromal cell-derived factor 1, were detected in both *Notch2*$^{tm1.1Ecan}$ and control serum, although there was no significant difference between genotypes (data not shown). These findings coincide with the RNA analysis of *Notch2*$^{tm1.1Ecan}$ BMMs, where the induction of inflammatory cytokines was comparable between *Notch2*$^{tm1.1Ecan}$ and control cells and observed only after TNFα stimulation. These observations suggest that TNFα is required for *Notch2*$^{tm1.1Ecan}$ mice to exhibit an inflammatory response. However, the circumstances leading to a possible increase in local or systemic TNFα in subjects afflicted by HCS are not known.

It has been an issue of controversy whether TNFα has direct effects on osteoclastogenesis or whether it requires RANKL to

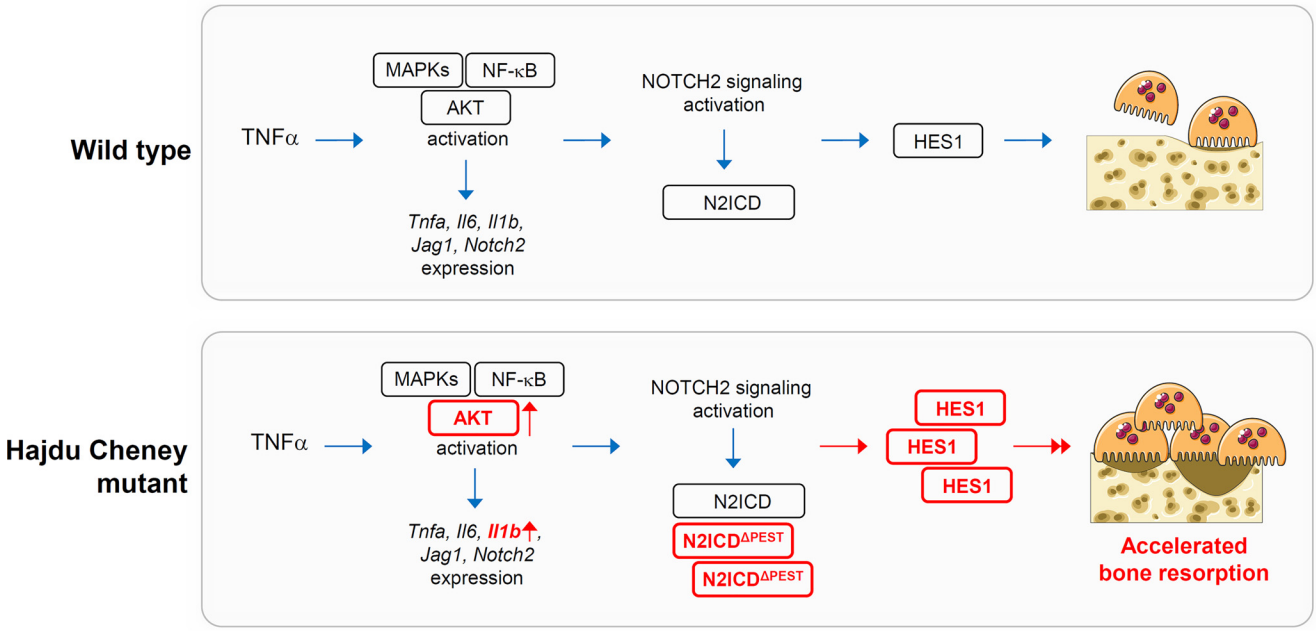

Figure 10. Schematic model to show the effects of the Hajdu Cheney mutation on TNFα-induced osteolysis. The *blue arrows* indicate signal activation. The *red arrows* and *boxes in bold* represent increased signal activation and expression in Hajdu Cheney mutants.

exert its actions (59). In this work, we did not detect *Tnfsf11* (encoding RANKL) in BMM cultures, treated or not, with TNFα (data not shown) suggesting that the effects observed were secondary to the direct actions of TNFα and not mediated by RANKL. Moreover, there was no difference on the induction of *Tnfsf11* by TNFα in *Notch2*$^{tm1.1Ecan}$ and control osteoblasts (data not shown) so that a differential expression of RANKL does not explain the phenotypic changes observed in *Notch2*$^{tm1.1Ecan}$ mutant mice under the influence of TNFα.

In conclusion, *Notch2*$^{tm1.1Ecan}$ mice are sensitized to the actions of TNFα on osteoclastogenesis and bone resorption, possibly explaining the acro-osteolysis observed in individuals affected by HCS.

Experimental procedures

Mice and TNFα-induced osteolysis in vivo

Notch2$^{tm1.1Ecan}$ mice harboring a 6955C→T substitution in the *Notch2* locus have been characterized in previous studies (5, 25, 46). Genotyping was conducted in tail DNA extracts by PCR using forward primer *Nch2Lox* gtF 5′-CCCTTCTCTCTGTGCGGTAG-3′ and reverse primer *Nch2Lox* gtR 5′-CTCAGAGCCAAAGCCTCACTG-3′ (Integrated DNA Technologies; IDT, Coralville, IA). *Hes1*$^{loxP/loxP}$ mice, where *loxP* sequences are knocked into the first intron and downstream of the 3′UTR of *Hes1* alleles, were obtained from RIKEN (Wako Saitama, Japan) (60). Genotyping was performed using forward primer 5′-CAGCCAGTGTCAACACGACACCGGACAAAC-3′ and reverse primer 5′-TCGCCTTCGCCTCTTCTCCATGATA-3′ (IDT).

Two-month-old heterozygous male *Notch2*$^{tm1.1Ecan}$ mice in a C57BL/6 background and control sex-matched littermates were administered TNFα, at a dose of 2 μg, or PBS by injection in the subcutaneous space over the calvarial vault once a day for 4 consecutive days and sacrificed 24 h after the last injection as reported previously (61). TNFα cDNA and expression vector were obtained from S. Lee (Farmington, CT), and TNFα was purified using nickel-nitrilotriacetic acid–agarose columns (Qiagen, Germantown, MD), in accordance with manufacturer's instructions. To test whether the effect of TNFα on osteolysis in *Notch2*$^{tm1.1Ecan}$ calvariae can be reversed by blocking NOTCH2 activation, antibodies directed to the NRR of NOTCH2 (anti-NOTCH2 NRR) or control anti-ragweed antibodies at a dose of 10 mg/kg (all from Genentech, South San Francisco, CA) (46) were injected with TNFα at a dose of 2 μg over the calvarial vault of male *Notch2*$^{tm1.1Ecan}$ mice and sex-matched littermate controls. All animal experiments were approved by the Institutional Animal Care and Use Committee of UConn Health.

Bone histomorphometry

Calvariae were excised and fixed in 10% formalin for 3 days, decalcified in 14% EDTA (pH 7.2) for 7 days, and embedded in paraffin. Histomorphometry of the medial aspect of each calvaria was carried out in 7-μm-thick sections stained with TRAP and hematoxylin (Thermo Fisher Scientific, Waltham, MA). TRAP enzyme histochemistry was conducted using a commercial kit (Sigma), in accordance with manufacturer's instructions. Stained sections were used to outline bone tissue area and to measure osteoclast number and surface as well as eroded surface at a magnification of ×100 using an OsteoMeasure morphometry system (Osteometrics, Atlanta, GA) (62).

BMM, adenovirus-Cre-mediated gene deletion, and osteoclast formation

To obtain BMMs, the marrow from heterozygous male *Notch2*$^{tm1.1Ecan}$ mutant and control sex-matched littermate mice was removed by flushing with a 26-gauge needle, and erythrocytes were lysed in 150 mM NH_4Cl, 10 mM $KHCO_3$ and

Table 1
Primers used for qRT-PCR determinations
GenBank™ accession numbers identify transcript recognized by primer pairs.

Gene	Strand	Sequence	GenBank™ accession no.
Acp5	Forward	5′-GACAAGAGGTTCCAGGAGAC-3′	NM_001102404; NM_001102405; NM_007388
	Reverse	5′-TTCCAGCCAGCACATACC-3′	
Ctsk	Forward	5′-AGATATTGGTGGCTTTGGAA-3′	NM_007802
	Reverse	5′-AACGAGAGGAGAAATGAAACA-3′	
Hes1	Forward	5′-ACCAAAGACGGCCTCTGAGCACAGAAAGT-3′	NM_008235
	Reverse	5′-ATTCTTGCCCTTCGCCTCTT-3′	
Il1b	Forward	5′-GGACAGAATATCAACCAACAAGTG-3′	NM_008361
	Reverse	5′-TCGTTGCTTGGTTCTCCTT-3′	
Il6	Forward	5′-CGGCCTTCCCTACTTCACAAGTCCG-3′	NM_001314054; NM_031168
	Reverse	5′-CAGGTCTGTTGGGAGTGGTATCC-3′	
Jag1	Forward	5′-TGGGAACTGTTGTGGTGGAGTCCG-3′	NM_013822
	Reverse	5′-GTGACGCGGGACTGATACTCCT-3′	
Nfatc1	Forward	5′-GCGCAAGTACAGTCTCAATGGCC-3′	NM_198429; NM_001164110; NM_001164111; NM_001164112; NM_00116641091; NM_016791
	Reverse	5′-GGATGGTGTGGGTGAGTGGT-3′	
Notch2	Forward	5′-TGACGTTGATGAGTGTATCTCCAAGCC-3′	NM_010928
	Reverse	5′-GTAGCTGCCCTGAGTGTTGTGG-3′	
Rpl38	Forward	5′-AGAACAAGGATAATGTGAAGTTCAAGGTTC-3′	NM_001048057; NM_001048058; NM_023372
	Reverse	5′-CTGCTTCAGCTTCTCTGCCTTT-3′	
Tnfa	Forward	5′-CCACCATCAAGGACTCAAATGG-3′	NM_001278601; NM_013693
	Reverse	5′-CCTTTGCAGAACTCAGGAATGGACATTCG-3′	
Tnfr1	Forward	5′-GGTCTGCTGATGTTAGGA-3′	NM_011609
	Reverse	5′-CTTGGCATCTCTTTGTAGG-3′	
Tnfr2	Forward	5′-TGTTCTTGTCTCAGTTTGTAGGG-3′	NM_011610
	Reverse	5′-AGTCGTCCTTCTCACCTCTT-3′	

0.1 mM EDTA (pH 7.4), as described previously (46). Cells were centrifuged, and the sediment was suspended in α-minimum essential medium (α-MEM) in the presence of 10% fetal bovine serum (FBS; both from Thermo Fisher Scientific) and recombinant human M-CSF at 30 ng/ml. M-CSF cDNA and expression vector were obtained from D. Fremont (St. Louis, MO), and M-CSF was purified as reported previously (63). Cells were seeded on plastic Petri dishes at a density of 300,000 cells/cm^2 and cultured for 3 days.

For osteoclast formation, cells were collected following treatment with 0.25% trypsin/EDTA for 5 min and seeded on tissue culture plates at a density of 62,500 cells/cm^2 in α-MEM with 10% FBS, M-CSF at 30 ng/ml, and TNFα at 50, 100, or 200 ng/ml, respectively. Cultures were carried out until the formation of multinucleated TRAP-positive cells. TRAP-positive cells containing more than three nuclei were considered osteoclasts. To test whether the effect of TNFα on osteoclastogenesis in *Notch2*$^{tm1.1Ecan}$ BMMs depended on NOTCH2 activation, anti-NOTCH2 NRR at 10 μg/ml, anti-JAG1 antibodies at 20 μg/ml, or control anti-ragweed antibodies at 10 or 20 μg/ml (all from Genentech) were added directly to the culture medium (45–47).

To inactivate *Hes1* in osteoclast precursors in the context of the *Notch2*$^{tm1.1Ecan}$ mutation, *Hes1*$^{loxP/loxP}$ alleles were introduced into *Notch2*$^{tm1.1Ecan}$ mice to create heterozygous *Notch2*$^{tm1.1Ecan}$;*Hes1*$^{loxP/loxP}$ mice. *Notch2*$^{tm1.1Ecan}$;*Hes1*$^{loxP/loxP}$ mice were crossed with *Hes1*$^{loxP/loxP}$ mice to obtain *Notch2*$^{tm1.1Ecan}$;*Hes1*$^{loxP/loxP}$ and *Hes1*$^{loxP/loxP}$ control littermates for study. BMMs from both cohorts were cultured in the presence of M-CSF at 30 ng/ml and TNFα at 200 ng/ml for 3 days. The cells were transduced with adenoviruses carrying cytomegalovirus (CMV)-Cre or CMV-GFP as control at a multiplicity of infection (m.o.i.) of 100 and cultured with M-CSF and TNFα for three additional days until formation of multinucleated TRAP-positive cells.

Quantitative RT-PCR (qRT-PCR)

Total RNA was extracted from osteoclasts with the RNeasy kit (Qiagen, Valencia, CA) and from homogenized calvarial bones with the micro-RNeasy kit (Qiagen), in accordance with manufacturer's instructions. The integrity of the RNA extracted from bones was assessed by microfluidic electrophoresis on an Experion system (Bio-Rad), and RNA with a quality indicator number equal to or higher than 7.0 was used for subsequent analysis. Equal amounts of RNA were reverse-transcribed using the iScript RT-PCR kit (Bio-Rad) and amplified in the presence of specific primers (all primers were from IDT; Table 1) with the SsoAdvanced™ Universal SYBR Green Supermix (Bio-Rad) at 60 °C for 40 cycles. Transcript copy number was estimated by comparison with a serial dilution of cDNA for *Acp5*, *Ctsk*, *Il1b, Il6, Jag1, Notch2,* and *Tnfa* (all from Thermo Fisher Scientific), *Hes1* (American Type Culture Collection (ATCC), Manassas, VA), and *Nfatc1* (Addgene plasmid 11793 created by A. Rao, La Jolla, CA).

The level of *Notch2*$^{6955C\rightarrow T}$ mutant transcript was measured as described previously (5). Total RNA was reverse-transcribed with Moloney murine leukemia virus reverse transcriptase in the presence of reverse primers for *Notch2* and *Rpl38* (Table 1). *Notch2* cDNA was amplified by qPCR in the presence of TaqMan gene expression assay mix, including specific primers (5′-CATCGTGACTTTCCA-3′ and 5′-GGATCTGGTACATAGAG-3′) and a 6-carboxyfluorescein–labeled DNA probe of sequence 5′-CATTGCCTAGGCAGC-3′ covalently attached to a 3′-minor groove binder quencher (Thermo Fisher Scientific), and SsoAdvanced Universal Probes Supermix (Bio-Rad) at 60 °C for 45 cycles (59). *Notch2*$^{6955C\rightarrow T}$ transcript copy number was estimated by comparison with a serial dilution of a synthetic DNA fragment (IDT) containing ~200 bp surrounding the 6955C→T mutation in the *Notch2* locus, and cloned into pcDNA3.1(−) (Thermo Fisher Scientific) by isothermal

single reaction assembly using commercially available reagents (New England Biolabs, Ipswich, MA) (60).

Amplification reactions were conducted in CFX96 qRT-PCR detection systems (Bio-Rad), and fluorescence was monitored during every PCR cycle at the annealing step. Data are expressed as copy number or relative expression corrected for *Rpl38* expression estimated by comparison with a serial dilution of cDNA for *Rpl38* (ATCC) (64).

Immunoblotting

TNFα-treated BMMs or osteoclasts from control or *Notch2*$^{tm1.1Ecan}$ mice were extracted in buffer containing 25 mM Tris-HCl (pH 7.5), 150 mM NaCl, 5% glycerol, 1 mM EDTA, 0.5% Triton X-100, 1 mM sodium orthovanadate, 10 mM NaF, 1 mM phenylmethylsulfonyl fluoride and a protease inhibitor mixture (all from Sigma). Quantified total cell lysates (35 μg of total protein) were separated by SDS-PAGE in 8 or 10% polyacrylamide gels and transferred to Immobilon-P membranes (Millipore, Billerica, MA). The blots were probed with anti-p-IκBα (9246), IκBα (9242), p-p38 (9211), p38 (9212), p-ERK (9101), ERK (9102), p-JNK (4668), JNK (9252), p-AKT (9271), AKT (9272) HES1 (11988), and β-Actin (3700) antibodies (all from Cell Signaling Technology, Danvers, MA). Anti-NOTCH2 (C651.6DbHN) and anti-JAG1 (TS1.15H) antibodies were obtained from Developmental Studies Hybridoma Bank (DSHB C651.6DbHN, University of Iowa, Iowa City). Anti-NFATc1 antibody (556602) was obtained from BD Biosciences. The blots were exposed to anti-rabbit IgG, anti-rat IgG, or anti-mouse IgG conjugated to horseradish peroxidase (Sigma) and incubated with a chemiluminescence detection reagent (Bio-Rad). Chemiluminescence was detected by ChemiDoc™ XSR+ molecular imager (Bio-Rad) with Image Lab™ software (version 5.2.1) (65), and the amount of protein in individual bands was quantified.

NF-κB activation assay

TNFα-treated BMMs from control or *Notch2*$^{tm1.1Ecan}$ mice were lysed prior to nuclear extraction using the nuclear extract kit (Active Motif, Inc., Carlsbad, CA). To detect and quantify NF-κB activation, 20 μg of nuclear extract samples were examined using a commercial ELISA-based kit (TransAM™ Flexi NF-κB p65, Active Motif, Inc.) (66), in accordance with manufacturer's instructions. Briefly, nuclear extracts were incubated with a biotinylated consensus NF-κB–binding sequence (5′-GGGACTTTCC-3′) (1 pmol/well), and the reaction mixtures were transferred into assay wells. Subsequently, samples were incubated with anti-NF-κB p65 antibody, and anti-rabbit IgG was conjugated to horseradish peroxidase and developed, and colorimetric changes were measured in an iMark™ Microplate Absorbance Reader (Bio-Rad) at 450 nm with a reference wavelength of 655 nm. To assess the specificity of NF-κB binding to the biotinylated probe, unlabeled WT or mutated consensus NF-κB binding oligonucleotide was added in excess (10 pmol/well) to the reaction mixture.

Serum TNFα

Serum levels of TNFα were measured in 2- and 12-month-old *Notch2*$^{tm1.1Ecan}$ male mice and control littermates using a mouse TNFα-uncoated enzyme-linked immunosorbent assay kit in accordance with manufacturer's instructions (Thermo Fisher Scientific; catalogue 88-7324).

Statistics

Data are expressed as means ± S.D. Statistical differences were determined by Student's *t* test or two-way analysis of variance with Holm-Šídák post hoc analysis for pairwise or multiple comparisons, respectively.

Author contributions—J. Y. and E. C. conceptualization; J. Y. formal analysis; J. Y. and E. C. methodology; J.Y. writing-original draft; E. C. supervision; E. C. funding acquisition; E. C. project administration; E. C. writing-review and editing.

Acknowledgments—We thank Genentech for anti-NOTCH2 NRR, anti-JAG1, and control anti-ragweed antibodies; S. Lee for TNFα cDNA; D. Fremont for M-CSF cDNA; M. Glogauer for Tnfsf11 cDNA; A. Rao for Nfatc1 cDNA; Lauren Schilling and Tabitha Eller for technical assistance; and Mary Yurczak for secretarial support.

References

1. Siebel, C., and Lendahl, U. (2017) Notch signaling in development, tissue homeostasis, and disease. *Physiol. Rev.* **97,** 1235–1294 CrossRef Medline
2. Zanotti, S., and Canalis, E. (2016) Notch signaling and the skeleton. *Endocr. Rev.* **37,** 223–253 CrossRef Medline
3. Bai, S., Kopan, R., Zou, W., Hilton, M. J., Ong, C. T., Long, F., Ross, F. P., and Teitelbaum, S. L. (2008) NOTCH1 regulates osteoclastogenesis directly in osteoclast precursors and indirectly via osteoblast lineage cells. *J. Biol. Chem.* **283,** 6509–6518 CrossRef Medline
4. Canalis, E., Parker, K., Feng, J. Q., and Zanotti, S. (2013) Osteoblast lineage-specific effects of notch activation in the skeleton. *Endocrinology* **154,** 623–634 CrossRef Medline
5. Canalis, E., Schilling, L., Yee, S. P., Lee, S. K., and Zanotti, S. (2016) Hajdu Cheney mouse mutants exhibit osteopenia, increased osteoclastogenesis and bone resorption. *J. Biol. Chem.* **291,** 1538–1551 CrossRef Medline
6. Canalis, E., Yu, J., Schilling, L., Yee, S. P., and Zanotti, S. (2018) The lateral meningocele syndrome mutation causes marked osteopenia in mice. *J. Biol. Chem.* **293,** 14165–14177 CrossRef Medline
7. Fukushima, H., Nakao, A., Okamoto, F., Shin, M., Kajiya, H., Sakano, S., Bigas, A., Jimi, E., and Okabe, K. (2008) The association of Notch2 and NF-κB accelerates RANKL-induced osteoclastogenesis. *Mol. Cell. Biol.* **28,** 6402–6412 CrossRef Medline
8. Hilton, M. J., Tu, X., Wu, X., Bai, S., Zhao, H., Kobayashi, T., Kronenberg, H. M., Teitelbaum, S. L., Ross, F. P., Kopan, R., and Long, F. (2008) Notch signaling maintains bone marrow mesenchymal progenitors by suppressing osteoblast differentiation. *Nat. Med.* **14,** 306–314 CrossRef Medline
9. Zanotti, S., and Canalis, E. (2017) Parathyroid hormone inhibits Notch signaling in osteoblasts and osteocytes. *Bone* **103,** 159–167 CrossRef Medline
10. Lindsell, C. E., Boulter, J., diSibio, G., Gossler, A., and Weinmaster, G. (1996) Expression patterns of Jagged, Delta1, Notch1, Notch2, and Notch3 genes identify ligand-receptor pairs that may function in neural development. *Mol. Cell. Neurosci.* **8,** 14–27 CrossRef Medline
11. Canalis, E. (2018) Notch in skeletal physiology and disease. *Osteoporos. Int.* **29,** 2611–2621 CrossRef Medline
12. Sanchez-Irizarry, C., Carpenter, A. C., Weng, A. P., Pear, W. S., Aster, J. C., and Blacklow, S. C. (2004) Notch subunit heterodimerization and prevention of ligand-independent proteolytic activation depend, respectively, on a novel domain and the LNR repeats. *Mol. Cell. Biol.* **24,** 9265–9273 CrossRef Medline
13. Iso, T., Kedes, L., and Hamamori, Y. (2003) HES and HERP families: multiple effectors of the Notch signaling pathway. *J. Cell. Physiol.* **194,** 237–255 CrossRef Medline

14. Iso, T., Sartorelli, V., Poizat, C., Iezzi, S., Wu, H. Y., Chung, G., Kedes, L., and Hamamori, Y. (2001) HERP, a novel heterodimer partner of HES/E(spl) in Notch signaling. *Mol. Cell. Biol.* **21,** 6080–6089 CrossRef Medline
15. Hajdu, N., and Kauntze, R. (1948) Cranio-skeletal dysplasia. *Br. J. Radiol.* **21,** 42–48 CrossRef Medline
16. Cheney, W. D. (1965) Acro-Osteolysis. *Am. J. Roentgenol. Radium. Ther. Nucl. Med.* **94,** 595–607 Medline
17. Canalis, E., and Zanotti, S. (2014) Hajdu-Cheney syndrome: a review. *Orphanet J. Rare Dis.* **9,** 200 CrossRef Medline
18. Gray, M. J., Kim, C. A., Bertola, D. R., Arantes, P. R., Stewart, H., Simpson, M. A., Irving, M. D., and Robertson, S. P. (2012) Serpentine fibula polycystic kidney syndrome is part of the phenotypic spectrum of Hajdu-Cheney syndrome. *Eur. J. Hum. Genet.* **20,** 122–124 CrossRef Medline
19. Isidor, B., Lindenbaum, P., Pichon, O., Bézieau, S., Dina, C., Jacquemont, S., Martin-Coignard, D., Thauvin-Robinet, C., Le Merrer, M., Mandel, J. L., David, A., Faivre, L., Cormier-Daire, V., Redon, R., and Le Caignec, C. (2011) Truncating mutations in the last exon of NOTCH2 cause a rare skeletal disorder with osteoporosis. *Nat. Genet.* **43,** 306–308 CrossRef Medline
20. Majewski, J., Schwartzentruber, J. A., Caqueret, A., Patry, L., Marcadier, J., Fryns, J. P., Boycott, K. M., Ste-Marie, L. G., McKiernan, F. E., Marik, I., Van Esch, H., FORGE Canada Consortium, Michaud, J. L., and Samuels, M. E. (2011) Mutations in NOTCH2 in families with Hajdu-Cheney syndrome. *Hum. Mutat.* **32,** 1114–1117 CrossRef Medline
21. Simpson, M. A., Irving, M. D., Asilmaz, E., Gray, M. J., Dafou, D., Elmslie, F. V., Mansour, S., Holder, S. E., Brain, C. E., Burton, B. K., Kim, K. H., Pauli, R. M., Aftimos, S., Stewart, H., Kim, C. A., *et al.* (2011) Mutations in NOTCH2 cause Hajdu-Cheney syndrome, a disorder of severe and progressive bone loss. *Nat. Genet.* **43,** 303–305 CrossRef Medline
22. Zhao, W., Petit, E., Gafni, R. I., Collins, M. T., Robey, P. G., Seton, M., Miller, K. K., and Mannstadt, M. (2013) Mutations in NOTCH2 in patients with Hajdu-Cheney syndrome. *Osteoporos. Int.* **24,** 2275–2281 CrossRef Medline
23. Fukushima, H., Shimizu, K., Watahiki, A., Hoshikawa, S., Kosho, T., Oba, D., Sakano, S., Arakaki, M., Yamada, A., Nagashima, K., Okabe, K., Fukumoto, S., Jimi, E., Bigas, A., Nakayama, K. I., *et al.* (2017) NOTCH2 Hajdu-Cheney mutations Escape SCF(FBW7)-dependent proteolysis to promote osteoporosis. *Mol. Cell* **68,** 645–658.e5 CrossRef Medline
24. Zanotti, S., Yu, J., Bridgewater, D., Wolf, J. M., and Canalis, E. (2018) Mice harboring a Hajdu Cheney syndrome mutation are sensitized to osteoarthritis. *Bone* **114,** 198–205 CrossRef Medline
25. Yu, J., Zanotti, S., Walia, B., Jellison, E., Sanjay, A., and Canalis, E. (2018) The Hajdu Cheney mutation is a determinant of B-cell allocation of the splenic marginal zone. *Am. J. Pathol.* **188,** 149–159 CrossRef Medline
26. Sakka, S., Gafni, R. I., Davies, J. H., Clarke, B., Tebben, P., Samuels, M., Saraff, V., Klaushofer, K., Fratzl-Zelman, N., Roschger, P., Rauch, F., and Högler, W. (2017) Bone structural characteristics and response to bisphosphonate treatment in children with Hajdu-Cheney syndrome. *J. Clin. Endocrinol. Metab.* **102,** 4163–4172 CrossRef Medline
27. Blumenauer, B. T., Cranney, A. B., and Goldstein, R. (2002) Acro-osteolysis and osteoporosis as manifestations of the Hajdu-Cheney syndrome. *Clin. Exp. Rheumatol.* **20,** 574–575 Medline
28. Brown, D. M., Bradford, D. S., Gorlin, R. J., Desnick, R. J., Langer, L. O., Jowsey, J., and Sauk, J. J. (1976) The acro-osteolysis syndrome: morphologic and biochemical studies. *J. Pediatr.* **88,** 573–580 CrossRef Medline
29. Udell, J., Schumacher, H. R., Jr, Kaplan, F., and Fallon, M. D. (1986) Idiopathic familial acroosteolysis: histomorphometric study of bone and literature review of the Hajdu-Cheney syndrome. *Arthritis Rheum.* **29,** 1032–1038 CrossRef Medline
30. Gu, Q., Yang, H., and Shi, Q. (2017) Macrophages and bone inflammation. *J. Orthop. Translat.* **10,** 86–93 CrossRef Medline
31. Kwan Tat, S., Padrines, M., Théoleyre, S., Heymann, D., and Fortun, Y. (2004) IL-6, RANKL, TNF-α/IL-1: interrelations in bone resorption pathophysiology. *Cytokine Growth Factor Rev.* **15,** 49–60 CrossRef Medline
32. Azuma, Y., Kaji, K., Katogi, R., Takeshita, S., and Kudo, A. (2000) Tumor necrosis factor-α induces differentiation of and bone resorption by osteoclasts. *J. Biol. Chem.* **275,** 4858–4864 CrossRef Medline
33. Komine, M., Kukita, A., Kukita, T., Ogata, Y., Hotokebuchi, T., and Kohashi, O. (2001) Tumor necrosis factor-α cooperates with receptor activator of nuclear factor κB ligand in generation of osteoclasts in stromal cell-depleted rat bone marrow cell culture. *Bone* **28,** 474–483 CrossRef Medline
34. Kobayashi, K., Takahashi, N., Jimi, E., Udagawa, N., Takami, M., Kotake, S., Nakagawa, N., Kinosaki, M., Yamaguchi, K., Shima, N., Yasuda, H., Morinaga, T., Higashio, K., Martin, T. J., and Suda, T. (2000) Tumor necrosis factor α stimulates osteoclast differentiation by a mechanism independent of the ODF/RANKL-RANK interaction. *J. Exp. Med.* **191,** 275–286 CrossRef Medline
35. Wei, S., Kitaura, H., Zhou, P., Ross, F. P., and Teitelbaum, S. L. (2005) IL-1 mediates TNF-induced osteoclastogenesis. *J. Clin. Invest.* **115,** 282–290 CrossRef Medline
36. Lee, Y. M., Fujikado, N., Manaka, H., Yasuda, H., and Iwakura, Y. (2010) IL-1 plays an important role in the bone metabolism under physiological conditions. *Int. Immunol.* **22,** 805–816 CrossRef Medline
37. Shiratori, T., Kyumoto-Nakamura, Y., Kukita, A., Uehara, N., Zhang, J., Koda, K., Kamiya, M., Badawy, T., Tomoda, E., Xu, X., Yamaza, T., Urano, Y., Koyano, K., and Kukita, T. (2018) IL-1β induces pathologically activated osteoclasts bearing extremely high levels of resorbing activity: a possible pathological subpopulation of osteoclasts, accompanied by suppressed expression of Kindlin-3 and Talin-1. *J. Immunol.* **200,** 218–228 CrossRef Medline
38. Axmann, R., Böhm, C., Krönke, G., Zwerina, J., Smolen, J., and Schett, G. (2009) Inhibition of interleukin-6 receptor directly blocks osteoclast formation *in vitro* and *in vivo*. *Arthritis Rheum.* **60,** 2747–2756 CrossRef Medline
39. Kotake, S., Sato, K., Kim, K. J., Takahashi, N., Udagawa, N., Nakamura, I., Yamaguchi, A., Kishimoto, T., Suda, T., and Kashiwazaki, S. (1996) Interleukin-6 and soluble interleukin-6 receptors in the synovial fluids from rheumatoid arthritis patients are responsible for osteoclast-like cell formation. *J. Bone Miner. Res.* **11,** 88–95 CrossRef Medline
40. Osta, B., Benedetti, G., and Miossec, P. (2014) Classical and paradoxical effects of TNF-α on bone homeostasis. *Front. Immunol.* **5,** 48 CrossRef Medline
41. Mbalaviele, G., Novack, D. V., Schett, G., and Teitelbaum, S. L. (2017) Inflammatory osteolysis: a conspiracy against bone. *J. Clin. Invest.* **127,** 2030–2039 CrossRef Medline
42. Zhao, B. (2017) TNF and bone remodeling. *Curr. Osteoporos. Rep.* **15,** 126–134 CrossRef Medline
43. Kim, J. H., Kim, A. R., Choi, Y. H., Jang, S., Woo, G. H., Cha, J. H., Bak, E. J., and Yoo, Y. J. (2017) Tumor necrosis factor-α antagonist diminishes osteocytic RANKL and sclerostin expression in diabetes rats with periodontitis. *PLoS ONE* **12,** e0189702 CrossRef Medline
44. Park, H. J., Baek, K., Baek, J. H., and Kim, H. R. (2017) TNFalpha increases RANKL expression via PGE(2)-induced activation of NFATc1. *Int. J. Mol. Sci.* **18,** E495 CrossRef Medline
45. Wu, Y., Cain-Hom, C., Choy, L., Hagenbeek, T. J., de Leon, G. P., Chen, Y., Finkle, D., Venook, R., Wu, X., Ridgway, J., Schahin-Reed, D., Dow, G. J., Shelton, A., Stawicki, S., Watts, R. J., *et al.* (2010) Therapeutic antibody targeting of individual Notch receptors. *Nature* **464,** 1052–1057 CrossRef Medline
46. Canalis, E., Sanjay, A., Yu, J., and Zanotti, S. (2017) An antibody to Notch2 reverses the osteopenic phenotype of Hajdu-Cheney mutant male mice. *Endocrinology* **158,** 730–742 CrossRef Medline
47. Lafkas, D., Shelton, A., Chiu, C., de Leon Boenig, G., Chen, Y., Stawicki, S. S., Siltanen, C., Reichelt, M., Zhou, M., Wu, X., Eastham-Anderson, J., Moore, H., Roose-Girma, M., Chinn, Y., Hang, J. Q., Warming, S., *et al.* (2015) Therapeutic antibodies reveal Notch control of transdifferentiation in the adult lung. *Nature* **528,** 127–131 CrossRef Medline
48. Vollersen, N., Hermans-Borgmeyer, I., Cornils, K., Fehse, B., Rolvien, T., Triviai, I., Jeschke, A., Oheim, R., Amling, M., Schinke, T., and Yorgan, T. A. (2018) High bone turnover in mice carrying a pathogenic Notch2

mutation causing Hajdu-Cheney syndrome. *J. Bone Miner. Res.* **33,** 70–83 CrossRef Medline
49. Zhao, B., Grimes, S. N., Li, S., Hu, X., and Ivashkiv, L. B. (2012) TNF-induced osteoclastogenesis and inflammatory bone resorption are inhibited by transcription factor RBP-J. *J. Exp. Med.* **209,** 319–334 CrossRef Medline
50. Zanotti, S., Smerdel-Ramoya, A., and Canalis, E. (2011) Hairy and enhancer of split (HES)1 is a determinant of bone mass. *J. Biol. Chem.* **286,** 2648–2657 CrossRef Medline
51. Shang, Y., Smith, S., and Hu, X. (2016) Role of Notch signaling in regulating innate immunity and inflammation in health and disease. *Protein Cell* **7,** 159–174 CrossRef Medline
52. Rechsteiner, M., and Rogers, S. W. (1996) PEST sequences and regulation by proteolysis. *Trends Biochem. Sci.* **21,** 267–271 CrossRef Medline
53. Cenciarelli, C., Marei, H. E., Zonfrillo, M., Casalbore, P., Felsani, A., Giannetti, S., Trevisi, G., Althani, A., and Mangiola, A. (2017) The interference of Notch1 target Hes1 affects cell growth, differentiation and invasiveness of glioblastoma stem cells through modulation of multiple oncogenic targets. *Oncotarget* **8,** 17873–17886 CrossRef Medline
54. Palomero, T., Sulis, M. L., Cortina, M., Real, P. J., Barnes, K., Ciofani, M., Caparros, E., Buteau, J., Brown, K., Perkins, S. L., Bhagat, G., Agarwal, A. M., Basso, G., Castillo, M., Nagase, S., *et al.* (2007) Mutational loss of PTEN induces resistance to NOTCH1 inhibition in T-cell leukemia. *Nat. Med.* **13,** 1203–1210 CrossRef Medline
55. Wong, G. W., Knowles, G. C., Mak, T. W., Ferrando, A. A., and Zúñiga-Pflücker, J. C. (2012) HES1 opposes a PTEN-dependent check on survival, differentiation, and proliferation of TCRbeta-selected mouse thymocytes. *Blood* **120,** 1439–1448 CrossRef Medline
56. Xie, S., Chen, M., Yan, B., He, X., Chen, X., and Li, D. (2014) Identification of a role for the PI3K/AKT/mTOR signaling pathway in innate immune cells. *PLoS ONE* **9,** e94496 CrossRef Medline
57. Lee, S. E., Woo, K. M., Kim, S. Y., Kim, H. M., Kwack, K., Lee, Z. H., and Kim, H. H. (2002) The phosphatidylinositol 3-kinase, p38, and extracellular signal-regulated kinase pathways are involved in osteoclast differentiation. *Bone* **30,** 71–77 CrossRef Medline
58. Ottaviani, S., Tahiri, K., Frazier, A., Hassaine, Z. N., Dumontier, M. F., Baschong, W., Rannou, F., Corvol, M. T., Savouret, J. F., and Richette, P. (2010) Hes1, a new target for interleukin 1β in chondrocytes. *Ann. Rheum. Dis.* **69,** 1488–1494 CrossRef Medline
59. Tanaka, S. (2017) RANKL-independent osteoclastogenesis: a long-standing controversy. *J. Bone Miner. Res.* **32,** 431–433 CrossRef Medline
60. Imayoshi, I., Shimogori, T., Ohtsuka, T., and Kageyama, R. (2008) Hes genes and neurogenin regulate non-neural versus neural fate specification in the dorsal telencephalic midline. *Development* **135,** 2531–2541 CrossRef Medline
61. Yeon Won, H., Hwan Mun, S., Shin, B., and Lee, S. K. (2016) Contradictory role of CD97 in basal and tumor necrosis factor-induced osteoclastogenesis *in vivo*. *Arthritis Rheumatol.* **68,** 1301–1313 CrossRef Medline
62. Dempster, D. W., Compston, J. E., Drezner, M. K., Glorieux, F. H., Kanis, J. A., Malluche, H., Meunier, P. J., Ott, S. M., Recker, R. R., and Parfitt, A. M. (2013) Standardized nomenclature, symbols, and units for bone histomorphometry: a 2012 update of the report of the ASBMR Histomorphometry Nomenclature Committee. *J. Bone Miner. Res.* **28,** 2–17 CrossRef Medline
63. Lee, S. H., Rho, J., Jeong, D., Sul, J. Y., Kim, T., Kim, N., Kang, J. S., Miyamoto, T., Suda, T., Lee, S. K., Pignolo, R. J., Koczon-Jaremko, B., Lorenzo, J., and Choi, Y. (2006) v-ATPase V0 subunit d2-deficient mice exhibit impaired osteoclast fusion and increased bone formation. *Nat. Med.* **12,** 1403–1409 CrossRef Medline
64. Kouadjo, K. E., Nishida, Y., Cadrin-Girard, J. F., Yoshioka, M., and St-Amand, J. (2007) Housekeeping and tissue-specific genes in mouse tissues. *BMC Genomics* **8,** 127 CrossRef Medline
65. Zanotti, S., Smerdel-Ramoya, A., and Canalis, E. (2013) Nuclear factor of activated T-cells (Nfat)c2 inhibits Notch signaling in osteoblasts. *J. Biol. Chem.* **288,** 624–632 CrossRef Medline
66. Sisto, M., Lisi, S., D'Amore, M., and Lofrumento, D. D. (2014) Rituximab-mediated Raf kinase inhibitor protein induction modulates NF-kappaB in Sjogren syndrome. *Immunology* **143,** 42–51 CrossRef Medline